Integration of space vector pulse width modulation controlled STATCOM with wind farm connected to multimachine power system

doi: http://dx.doi.org/10.1063/1.3049348

Integration of space vector pulse width modulation controlled STATCOM with wind farm connected to multimachine power system

S. M. Muyeen,[1,a)] Hany. M. Hasanien,[2] Rion Takahashi,[1] Toshiaki Murata,[1] and Junji Tamura[1]
[1]*Department of Electrical and Electronic Engineering, Kitami Institute of Technology, 165 Koen-cho, Kitami, 090-8507, Japan*
[2]*Department of Electrical Power and Machines, Ain Shams Univ., Cairo, Egypt*

(Received 26 August 2008; accepted 17 November 2008;
published online 23 December 2008)

In this work, dynamic and transient characteristics of a multimachine power system connected with two wind farms composed of fixed speed wind turbine generator systems (WTGS) are analyzed. At each wind farm the terminal one space vector pulse width modulation controlled voltage source converter based static synchronous compensator (STATCOM) is considered to be connected. The capacitor bank capacity of fixed speed wind generator is reduced by certain percentages when a STATCOM is integrated at a wind farm terminal. As wind speed is always fluctuating, the terminal voltage of a fixed speed wind generator also fluctuates randomly, which has an adverse effect on the rest of the power system. It is reported that the STATCOM with a reduced capacitor bank can decrease the voltage fluctuations of the multimachine power system as well as wind generator terminals. Moreover, it is shown that a STATCOM can also enhance the transient stability of induction and synchronous generators when a network disturbance occurs in the power system. Since shaft system modeling of a wind turbine has a significant effect on the transient stability analysis of WTGS, a two-mass shaft model is adopted in this study. Both of the symmetrical and the unsymmetrical faults are analyzed in light of the real wind farm grid code. The transient performance of a STATCOM on the network is evaluated by the transient stability index based on the total kinetic energy of generators. For dynamic performance evaluation, real wind speed data are used in the simulation. Finally, it is concluded that the STATCOM can enhance both dynamic and transient stability of wind farms connected with a multimachine power system. [DOI: 10.1063/1.3049348]

I. INTRODUCTION

Huge numbers of wind generators are going to be connected with the existing network in the near future. In 2007, 20 000 MW of wind power was installed all over the world, bringing worldwide installed capacity to 94 112 MW. This is an increase of 31% compared with the 2006 market and represents an overall increase in the global installed capacity of about 27%.[1] However, between the two types of popular trends though variable speed wind turbine generator systems (WTGS) are becoming more popular, the statistics show that the total installation of fixed speed WTGS is around 40%.[2] Therefore, it is still needed to analyze the stability characteristics of wind farm composed of fixed speed WTGS. Though output power fluctuation of a wind farm is a great problem for the transmission system operator (TSO) or power grid companies, this paper concentrates only on the voltage fluctuation and restoration issues of fixed speed wind farm.

[a)]Electronic mail: muyeen@pullout.elec.kitami-it.ac.jp.

Voltage or current source inverter based flexible alternating current (ac) transmission systems (FACTS) devices such as a static var compensator, static synchronous compensator (STATCOM), dynamic voltage restorer, solid state transfer switch, and unified power flow controller have been used for flexible power flow control, secure loading and damping of power system oscillation.[3–5] Some of the FACTS devices have been used to improve transient and dynamic stabilities of a wind generator. Induction generator (IG), in general, is widely used as a wind generator due to its simple, rugged, and maintenance free construction. However, as it has some stability problems,[6] it is necessary to investigate the stability aspect of induction generator when connected to the power grid. Some authors have reported valuable studies on the STATCOM connected with WTGS.[7–10] In Ref. 7, steady state reactive power control and islanding performance of an induction generator are discussed. Flicker mitigation of wind generator by using a STATCOM is discussed in Ref. 8 Though a lot of works with STATCOM have been reported so far, stability enhancement of WTGS by using the STATCOM is not sufficient enough. In Ref. 9, it is reported that a STATCOM can recover terminal voltage of a wound rotor induction generator after a fault clearance. But as only an induction generator is considered in the model network, the effect of the STATCOM on the rest of the system is not clarified there. In our previous work,[10] stability of a fixed speed WTGS connected to a grid is discussed, considering a phase modulation controlled voltage source converter (VSC) based STATCOM. The model system used therein is very simple which is composed of only one synchronous generator and infinite bus. The sinusoidal pulse width modulation (PWM) technique is considered therein. The sinusoidal PWM is a matured technology, which has been extensively used because it improves the voltage harmonic components to higher frequencies.[11–14] However, the space vector pulse width modulation (SVPWM) technique has been increasingly used in the last decade because it allows reducing commutation loss and the harmonic current of output voltage and obtains higher amplitude modulation indexes if compared with the conventional sinusoidal PWM technique.[13–15]

In this work, dynamic and transient stability of wind generators is analyzed in detail using a power system model in which two wind farms are connected with a multimachine (9 bus) power system. A two-level SVPWM based STATCOM is connected to each wind farm terminal. The well-known cascaded vector control scheme is used as the control methodology of the STATCOM. Since shaft system modeling has a significant effect on the transient stability of WTGS,[16,17] a two-mass shaft model is considered in this study. The capacitor bank capacity of the wind generator is reduced by 15% when the STATCOM is integrated at the wind farm terminal. As wind speed is intermittent and stochastic in nature, the terminal voltage of a fixed speed wind generator fluctuates randomly, which has an adverse effect on the rest of the power system. In this study, it is reported that the STATCOM with a reduced capacitor bank can decrease the voltage fluctuations of a multimachine power system as well as wind generator terminals. Moreover, it is shown that the STATCOM can enhance the transient stability of induction and synchronous generators when a network disturbance occurs in the power system. Both of the symmetrical and the unsymmetrical faults are considered as the network disturbances. Transient stability analysis is done in light of the real grid code suitable for wind farm.[18,19] The transient stability index based on the total kinetic energy of synchronous generators is considered in order to evaluate stabilization performance of the STATCOM. Finally, it is concluded that the STATCOM can enhance both of the dynamic and transient stability of fixed speed wind farms connected with multimachine power system.

II. WIND TURBINE MODELING

A mathematical relation for the mechanical power extraction from the wind can be expressed as follows:[20]

$$P_w = 0.5\rho\pi R^2 V_w^3 C_p(\lambda,\beta), \tag{1}$$

where P_w is the extracted power from the wind, ρ is the air density (kg/m^3), R is the blade radius (m), V_w is the wind speed (m/s), and C_p is the power coefficient which is a function of both tip

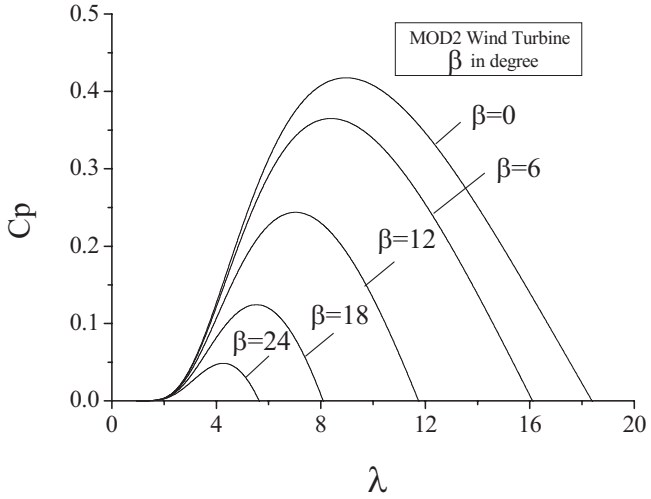

FIG. 1. C_p-λ curves for different pitch angles.

speed ratio, λ, and blade pitch angle, β (deg). In this work, the C_p equation as shown below[21] has been adopted

$$\lambda = \frac{V_w}{\omega_B}, \tag{2a}$$

$$C_p = \frac{1}{2}(\lambda - 0.022\beta^2 - 5.6)e^{-0.17\lambda}, \tag{2b}$$

where ω_B is the rotational speed (rad/s). The C_p-λ curves are shown in Fig. 1 for different values of β. A two-mass drive train model is used in this paper. A detailed description of the two-mass drive train model is shown in Ref. 17.

In this study, the conventional pitch controller shown in Fig. 2 is used. The purpose of using the pitch controller is to maintain the output power of the wind generator at rated level by controlling the blade pitch angle of the turbine blade when the wind speed is over the rated speed.

III. MODELING OF SPACE VECTOR PWM

The power electronic converter can operate only eight distinct topologies. Six out of these eight topologies produce a nonzero output voltage and are known active vectors ($\boldsymbol{V}_1 - \boldsymbol{V}_6$) and the remaining two topologies produce a zero output voltage and are known as zero vectors ($\boldsymbol{V}_0$, $\boldsymbol{V}_7$). The six active vectors are forming a regular hexagon and six sectors numbered **S-I** to **S-VI** in a stationary reference frame as shown in Fig. 3. Since the zero vectors have a zero magnitude and phase angle, the positions of these vectors are at origin as shown in Fig. 3.

The active vectors $\boldsymbol{V}_1 - \boldsymbol{V}_6$ are obtained as follows:

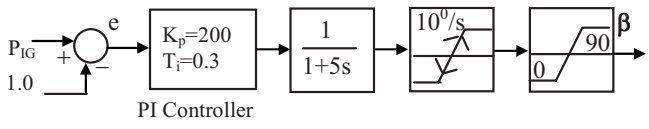

FIG. 2. Pitch controller.

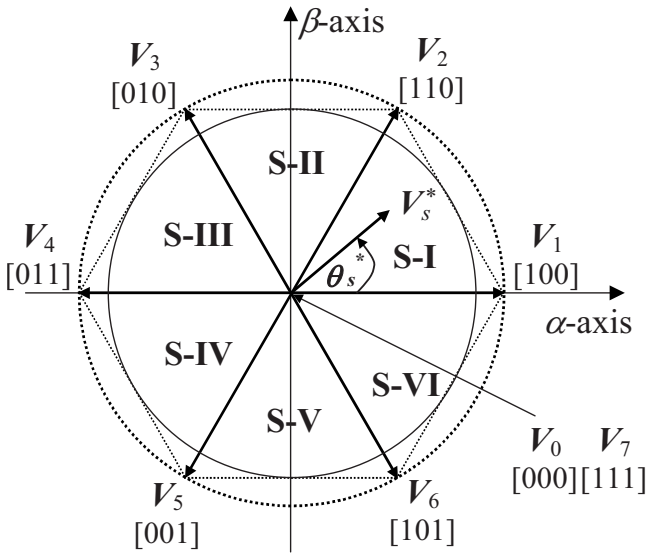

FIG. 3. Representation of the inverter states in the stationary reference frame.

$$\boldsymbol{V}_k = \sqrt{(2/3)} V_{\mathrm{dc}} e^{j(k-1)(\pi/3)}. \tag{3}$$

Here, $k=1,2,\ldots,6$.

It is seen from Eq. (3) that the magnitudes of all active vectors are the same and the angle between any adjacent two active vectors is 60 deg.

Let the desired voltage in a stationary (α-β axis) reference frame is $\boldsymbol{V}_s^*$. Then, the vector, magnitude, and angle of the desired voltage can be given as follows:

$$\boldsymbol{V}_s^* = |\boldsymbol{V}_s^*| e^{j\theta_s^*}, \tag{4}$$

$$\theta_s^* = \tan^{-1}[V_{s\beta}^*/V_{s\alpha}^*],$$

$$|\boldsymbol{V}_s^*| = \sqrt{V_{s\alpha}^{*2} + V_{s\beta}^{*2}}. \tag{5}$$

Looking at Fig. 3 one finds that, assuming $\mathbf{V}_s^*$ to be lying in sector k, the adjacent active vectors are $\boldsymbol{V}_k$ and $\boldsymbol{V}_{k+1}$. To achieve the desired stator voltage $\boldsymbol{V}_s^*$ within the sampling time T_s, the active voltage vectors $\boldsymbol{V}_k$ and $\boldsymbol{V}_{k+1}$ should be activated during the time T_k and T_{k+1}, respectively. Hence, the on-time T_k and T_{k+1} are evaluated by the following equations:

$$\boldsymbol{V}_s^* T_s = \boldsymbol{V}_k T_k + \boldsymbol{V}_{k+1} T_{k+1}. \tag{6}$$

Splitting this vectorial equation into real and imaginary components, from Eqs. (3)–(6) follows that:

$$\begin{bmatrix} T_k \\ T_{k+1} \end{bmatrix} = \frac{2}{\sqrt{3}} \frac{T_s |\boldsymbol{V}_s^*|}{k_T V_{\mathrm{dc}}} \begin{bmatrix} \sin\left[\dfrac{k\pi}{3} - \theta_s^*\right] \\ \sin\left[\theta_s^* - \dfrac{(k-1)\pi}{3}\right] \end{bmatrix}, \tag{7}$$

where the constant k_T is arbitrary and the value may be chosen equal to $2/3$ or $\sqrt{2/3}$.[22]

The on-time for the zero state vectors is obtained by the following equation:

$$T_0 = T_s - (T_k + T_{k+1}). \tag{8}$$

TABLE I. Sequence of selected vectors with respect to time.

Sector/time	$T_0/4$	$T_k/2$	$T_{k+1}/2$	$T_0/2$	$T_{k+1}/2$	$T_k/2$	$T_0/4$
S-I	V_0	V_1	V_2	V_7	V_2	V_1	V_0
S-II		V_3	V_2		V_2	V_3	
S-III		V_3	V_4		V_4	V_3	
S-IV		V_5	V_4		V_4	V_5	
S-V		V_5	V_6		V_6	V_5	
S-VI		V_1	V_6		V_6	V_1	

In order to obtain optimal harmonic performance and the minimum switching frequency for each of the power devices, the vector sequences are arranged such that the transition from one vector to the next is performed by switching only one converter leg. Therefore, the request minimum number of commutations per cycle is met if the active vectors are selected as Table I.

When $T_k+T_{k+1}>T_s$, the time T_k and T_{k+1} are simply rescaling as follows:

$$\begin{bmatrix} T'_k \\ T'_{k+1} \end{bmatrix} = \frac{T_s}{T_k + T_{k+1}} \begin{bmatrix} T_k \\ T_{k+1} \end{bmatrix}, \tag{9}$$

so that $T'_k+T'_{k+1}=T_s$ and $T_0=0$. According to this rescaling process, the converter can operate up to the modulation index 0.952. Applying the special switching in the SVM process of a PWM inverter the inverter, can be operated up to the modulation index 1.155.[15] In this work, the modeling of SVPWM is implemented by using PSCAD/EMTDC,[23] which is demonstrated in

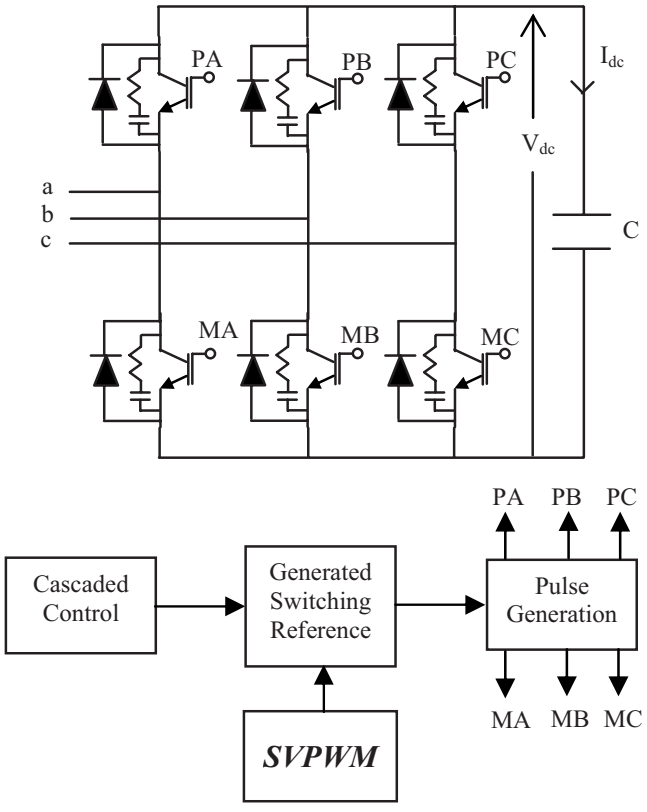

FIG. 4. Schematic diagram of a STATCOM switching circuit.

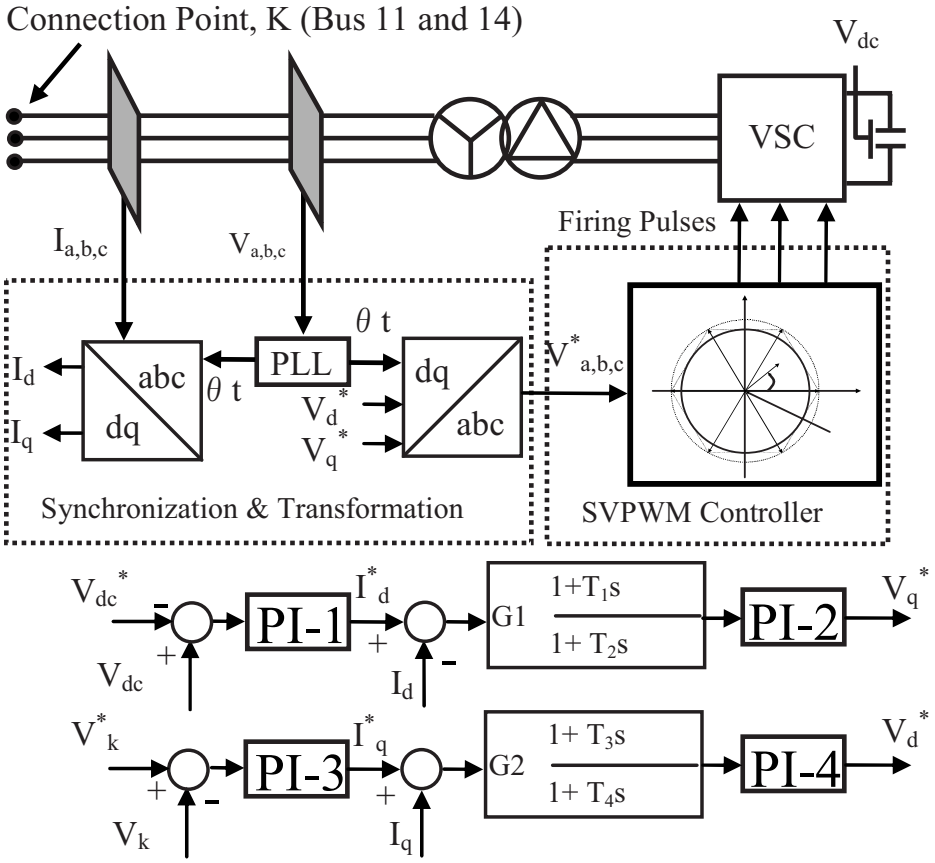

FIG. 5. Control block diagram of a VSC based STATCOM.

detail in our earlier work.[24] The reference voltage from the vector controlled VSC is progressed through the SVPWM controller to generate the switching signals for insulated-gate-bipolar-transistors (IGBT) of the STATCOM.

IV. STATCOM CONTROL STRATEGY

The schematic diagram of the STATCOM switching circuit is shown in Fig. 4. The aim of the control is to maintain the desired voltage magnitude at the wind farm terminals (Bus 11 and Bus

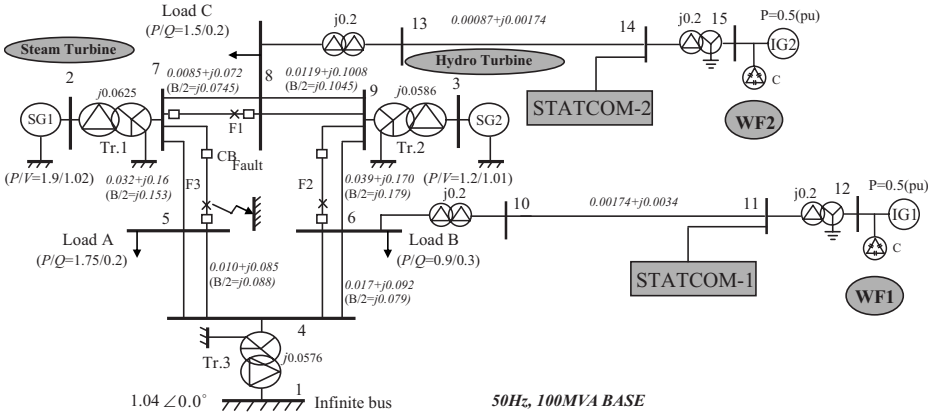

FIG. 6. Model system with a 9-bus main system and two wind farms.

TABLE II. Generator parameters.

	Synchronous			
	SG1	SG2	Induction generators	
MVA	200	130	**MVA**	**50**
r_a (pu)	0.003	0.003	$r1$ (pu)	0.01
x_a (pu)	0.102	0.130	$x1$ (pu)	0.1
X_d (pu)	1.651	1.200	*Xmu* (pu)	3.5
X_q (pu)	1.590	0.700	$r21$ (pu)	0.035
X'_d (pu)	0.232	0.300	$x21$ (pu)	0.030
X'_q (pu)	0.380		$r22$ (pu)	0.014
X''_d (pu)	0.171	0.220	$x22$ (pu)	0.098
X''_q (pu)	0.171	0.250	*Hg* (pu)	0.3
T'_{do} (s)	5.900	5.000	*Hwt* (pu)	3.0
T'_{qo} (s)	0.535		*Kw* (pu)	90
T''_{do} (s)	0.033	0.040		
T''_{qo} (s)	0.078	0.050		
H (s)	9.000	2.500		

14). Usually, wind farm terminal voltage is not kept constant to be the rated voltage, but reset to a desired value once or a few times a day by the TSO. For the control of the VSC, the well-known cascaded vector control scheme is used as shown in Fig. 5. The VSC converts the direct current (dc) voltage across the storage device into a set of three-phase ac output voltages. These voltages are supplied to the ac system through the impedance of the coupling transformer. The dq quantities and three-phase electrical quantities are related to each other by reference frame transformation. The angle of the transformation is detected from the three phase voltages (v_a, v_b, v_c) at each connection point of the STATCOM (Bus 11 and Bus 14) by using the phase locked loop system. Suitable adjustment of the phase and magnitude of the VSC output voltage allows the effective control of a power exchange between the STATCOM and the ac system. The vector control scheme generates the three-phase reference signals which are used to generate the switching signals for the IGBT switched VSC. In the simulation, the sampling time T_s of the SPVWM is chosen 0.001 s. The snubber circuit resistance and capacitance values of the IGBT devices shown in Fig. 4 are 5000 Ω and 0.05 μF, respectively. The VSC rating is considered to be the same as wind farm rating. To speed up the simulation though a 50 MVAr STATCOM consists of one inverter unit is considered in the simulation, practically it can be spilled into four 12.5 MVAr inverter units as shown in the Appendix. The rated dc link voltage is 5.5 kV. The STATCOM is connected to the 66 kV line by a single step down transformer (66 kV/3.2 kV) with 0.2 pu leakage reactance (base value 100 MVA). The dc-link capacitor value is 50 000 μF.

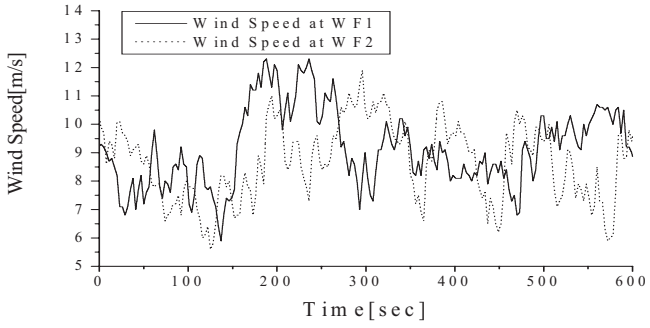

FIG. 7. Wind speed data for wind farms 1 and 2.

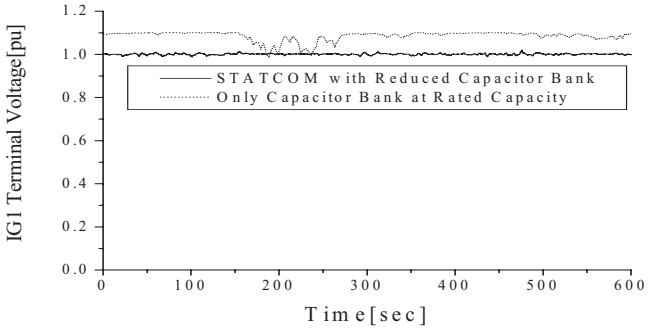

FIG. 8. Terminal voltage of IG1 with and without the STATCOM.

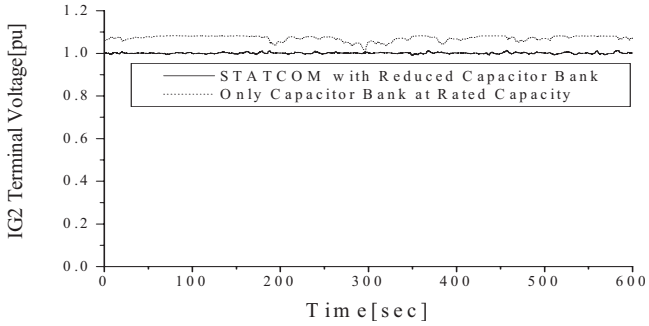

FIG. 9. Terminal voltage of IG2 with and without the STATCOM.

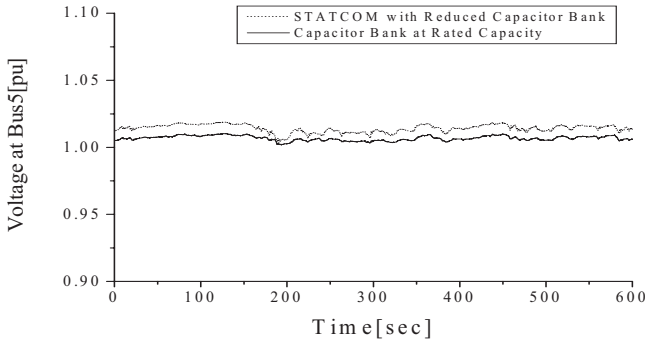

FIG. 10. Voltage at Bus-5 with and without the STATCOM.

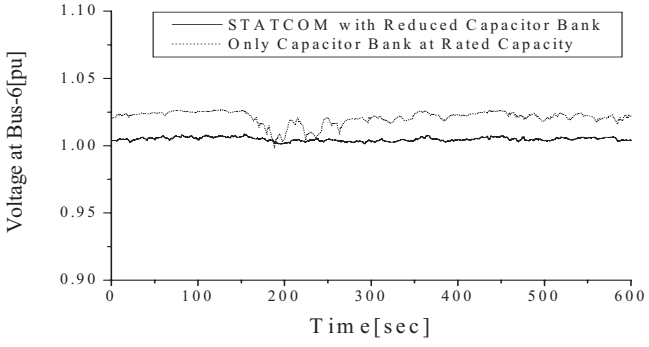

FIG. 11. Voltage at Bus-6 with and without the STATCOM.

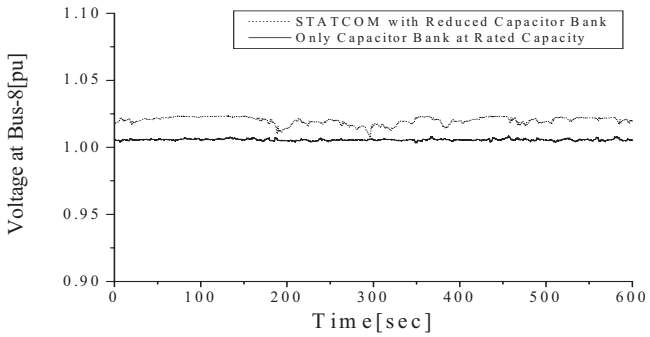

FIG. 12. Voltage at Bus-8 with and without the STATCOM.

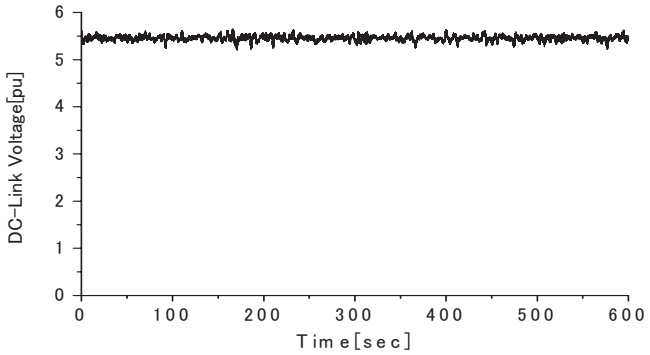

FIG. 13. dc-link voltage of the STATCOM.

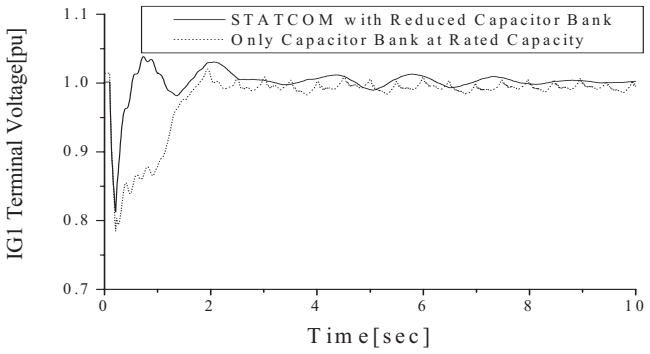

FIG. 14. Terminal voltage of IG1 with and without the STATCOM (3LG).

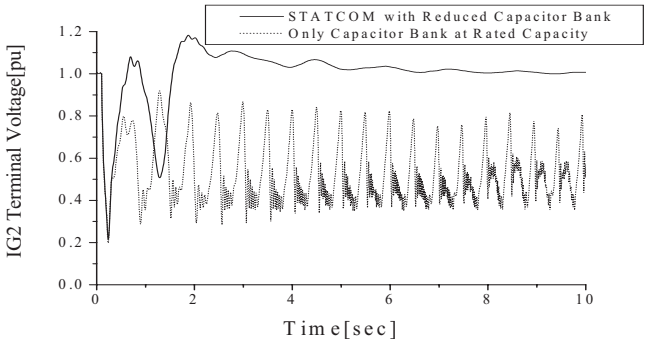

FIG. 15. Terminal voltage of IG2 with and without the STATCOM (3LG).

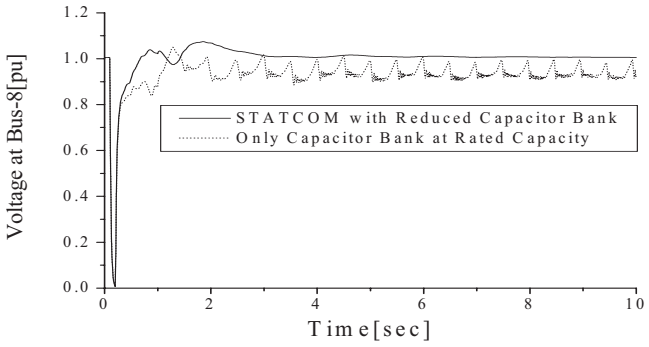

FIG. 16. Voltage at Bus-8 with and without the STATCOM (3LG).

V. MODEL SYSTEM

Figure 6 shows a model system with 9-bus main system and two wind farms. Steam and hydroturbine driven synchronous generators are connected with the main system as generator 1 and 2, respectively. The IEEE generic turbine model and approximate mechanical-hydraulic speed governing system[25] is used for synchronous generator 1 (SG1). The IEEE "nonelastic water column without surge tank" turbine model and "PID control including pilot and servo dynamics" speed-governing system[26] is used for synchronous generator 2 (SG2). IEEE alternator supplied rectifier excitation system[27] is used in the exciter model of both synchronous generators. Wind farms 1 and 2 are considered to be connected surrounding the hydrogenerator with long and short transmission lines, respectively. In both wind farms, induction generators are used as wind generators. Each wind farm has a power capacity of 50 MVA. It is assumed that several fixed-speed wind generators are lumped together to obtain the 50 MVA fixed-speed wind generator.[28] The generator parameters are shown in Table II, where base impedances for SG1, SG2, and induction generators are 2, 3.07, and 0.0095 Ω, respectively. For transmission line parameters shown in Fig. 6, system base 100 MVA, 500 kV are chosen. A capacitor bank C has been used for reactive power compensation of each IG at steady state. The value of capacitor C is chosen so that power factor of the wind power station during the rated operation becomes unity.[29] This capacitor bank value is reduced by 15% when the STATCOM is connected at each wind farm terminal.

VI. SIMULATION RESULTS

In this study, an aggregated wind farm model is considered, where several WTGSs are lumped together to obtain a large WTGS. The reason is that the detailed switching model is used in the simulation instead of the time average model of cascaded control of a SVPWM based STATCOM,

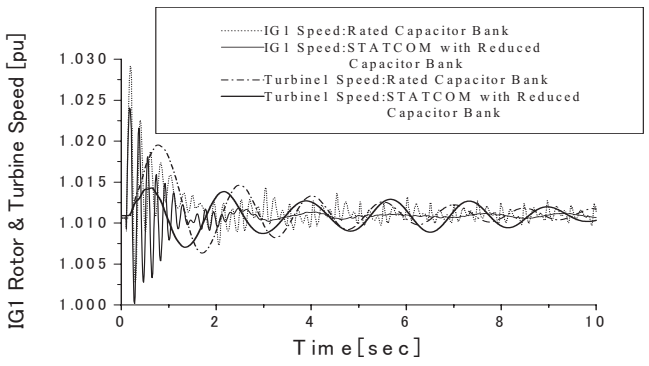

FIG. 17. Rotor and turbine speed of IG1 with and without the STATCOM (3LG).

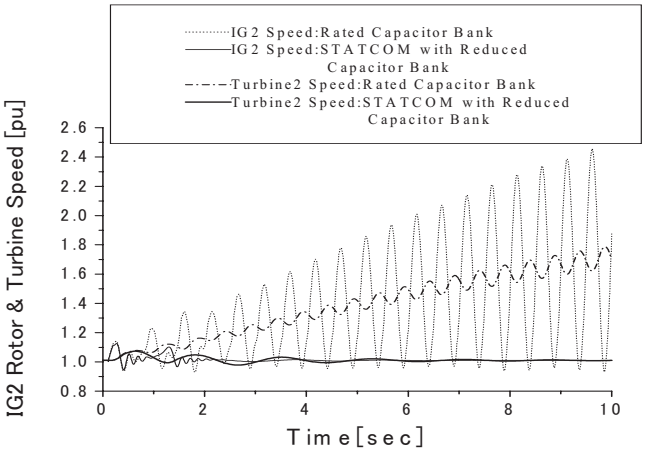

FIG. 18. Rotor and turbine speed of IG2 with and without the STATCOM (3LG).

which makes the simulation considerably slower. The simulation time step used in this study is 0.00002 s. For dynamic and transient analyses, the simulation time is chosen 600 and 10 s, respectively. Simulations have been done by using PSCAD/EMTDC.[23]

A. Dynamic characteristics analysis

Real wind speed data are shown in Fig. 7, which was obtained in Hokkaido Island, Japan, is used for each induction generator of wind farms 1 and 2. Though the wind speed is fluctuating randomly, the induction generator terminal voltages of wind farms 1 and 2 can be maintained constant when the STATCOM is used as shown in Figs. 8 and 9, respectively. Moreover, other bus voltages at Bus-5, 6, and 8 can also be maintained almost constant as shown in Figs. 10–12. The response of dc-link voltage is shown in Fig. 13. It is seen from the simulation results that the STATCOM even with a reduced capacitor bank can maintain the bus voltages at a desired level under randomly fluctuating wind conditions.

B. Transient performance analysis of the WTGS

The wind farm compatible grid code is more or less similar. The wind farm terminal voltage has to return to 90% of the nominal voltage within 3 s after the starting of a voltage drop.[18,19] Otherwise, the plant has to be shutdown. An induction generator requires large reactive power to recover the air gap flux when a short circuit fault occurs in the power system.[6] If sufficient reactive power is not supplied, then the electromagnetic torque of the wind generator decreases significantly with the decrease of the terminal voltage. Then the difference between mechanical and

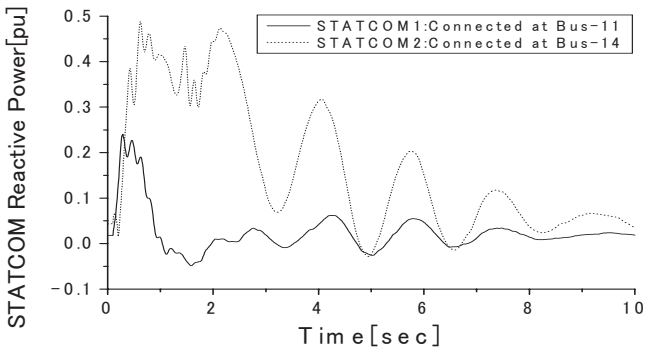

FIG. 19. Reactive power of STATCOM-1 and STATCOM-2 (3LG).

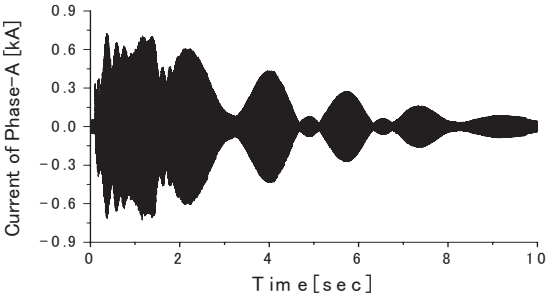

FIG. 20. Line current from STATCOM-2 to Bus-14 (3LG).

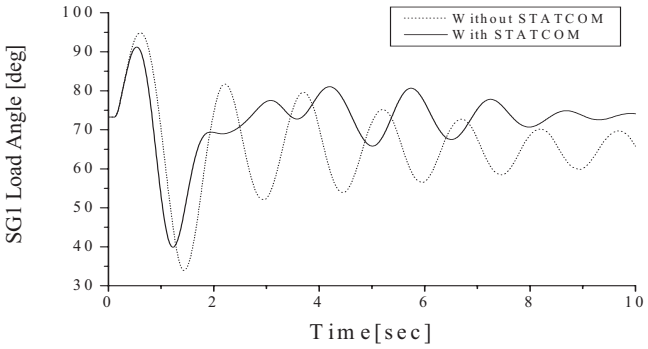

FIG. 21. Load angle of synchronous generator 1 (3LG).

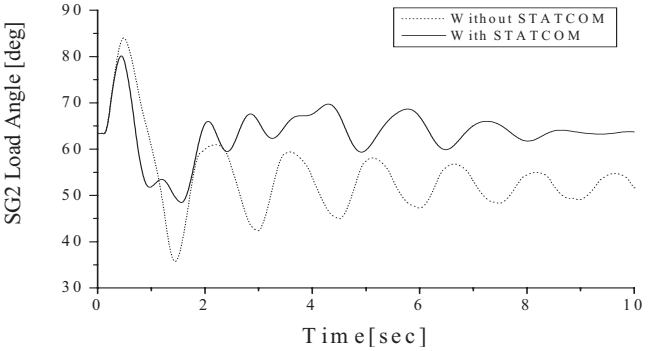

FIG. 22. Load angle of synchronous generator 2 (3LG).

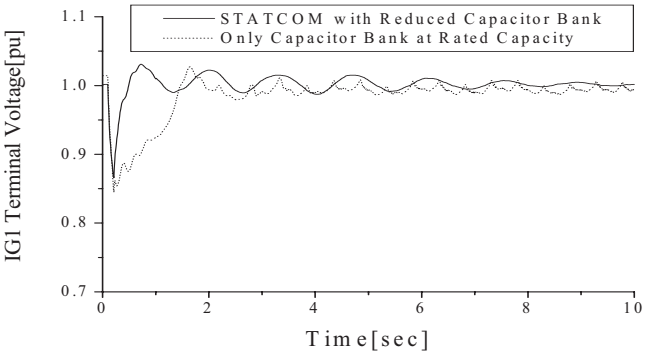

FIG. 23. Terminal voltage of IG1 with and without the STATCOM (2LG).

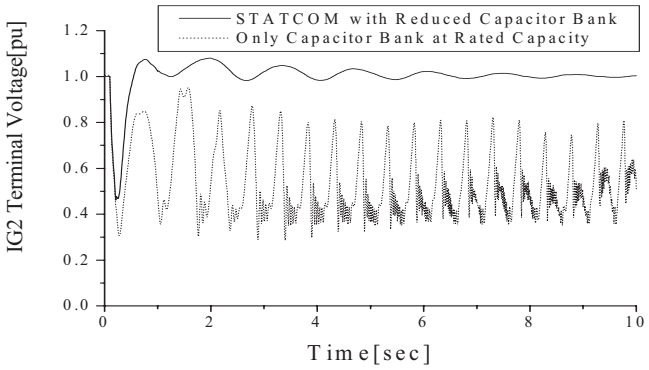

FIG. 24. Terminal voltage of IG2 with and without the STATCOM (2LG).

electromagnetic torques becomes large and the wind generator and turbine speeds increase rapidly. As a result, the induction generator becomes unstable and is requires to be disconnected from the power system. However, the recent trend is to decrease the shut down operation because a shut down of a large wind farm can have a serious effect on the power system operation. For transient characteristic analysis, the wind speed is kept constant at a rated speed, assuming that the wind speed does not change dramatically within the small time duration considered. At first, a three-line to ground fault (3LG) occurs at fault point F1 in Fig. 6 at time $t=0.1$ s, the faulted line is cleared at $t=0.2$ s, and the line is reclosed at $t=1.0$ s. Responses of terminal voltages at wind farms 1 and 2 are shown in Figs. 14 and 15, respectively. The voltage of Bus-8 is also shown in Fig. 16. The generator rotor and turbine hub speeds of WTGSs 1 and 2 are shown in Figs. 17 and 18. Reactive power responses of the two STATCOMs are shown in Fig. 19. As the fault occurs near wind farm 2, the capacitor bank installed at the terminal of IG2 cannot provide the necessary reactive power when a STATCOM is not considered. Therefore, IG2 becomes out of step and needs to shutdown as explained above. However, when a STATCOM is used, IG2 becomes stable and shutdown phenomenon can be avoided. Induction generator 1 is far away from the fault point and the terminal voltage decreases a little as shown in Fig. 14. Therefore, the mechanical and electromagnetic torque imbalance is small and IG1 becomes stable quickly with and without considering a STATCOM as shown in Fig. 17. The response of line current from STATCOM-2 to the connection point (Bus-14) is shown in Fig. 20. Responses of load angles of SG1 and SG2 are shown in Figs. 21 and 22, respectively. It is seen that a STATCOM can enhance the transient stability of synchronous generators as well as wind generators when the severe 3LG fault occurs in the power system.

Responses of terminal voltages of wind farms 1 and 2, when a two-line to ground fault (2LG) occurs from phase-B and phase-C to ground, are shown in Figs. 23 and 24 respectively. Reactive

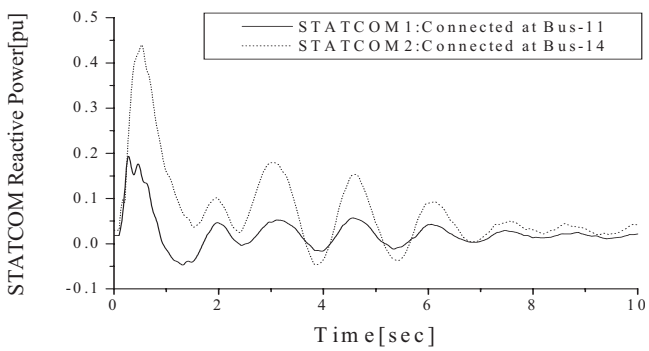

FIG. 25. Reactive power of STATCOM-1 and STATCOM-2 (2LG).

TABLE III. Transient stability index [W_c (s)] for 3LG fault.

Fault location	Only capacitor bank at rated capacity	STATCOM with reduced capacitor bank
F1	3.92	2.36
F2	3.20	1.58
F3	3.88	2.82

power responses of STATCOM-1 and STATCOM-2 are shown in Fig. 25. From these figures, it is clear that a STATCOM can also stabilize the wind generators under unsymmetrical faults. The system is found to be stable during single-line-to-ground fault with the capacitor bank at rated value, though the simulation results are not shown in this paper.

VII. TRANSIENT STABILITY EVALUATION

For the evaluation of transient stability, we used the stability index W_c (Ref. 30) as described below

$$W_c(\mathrm{s}) = \int_0^T \left| \frac{d}{dt} W_{\mathrm{total}} \right| dt \Big/ \text{system base power}, \tag{10}$$

where T is the simulation time of 10.0 s, W_{total} is the total kinetic energy which can be calculated easily by using the rotor speeds of the synchronous generators only and is given by

$$W_{\mathrm{total}} = \sum_{i=1}^{N} W_i \ (\mathrm{J}), \tag{11}$$

$$W_i = \frac{1}{2} J_i \omega_{mi}^2 \ (\mathrm{J}). \tag{12}$$

The smaller the value of W_c, the better the system's transient stability. The transient stability index with and without considering the STATCOM against 3LG fault is shown in Table III for different fault points of the model system. From Table III it can be easily understood that the SVPWM controlled STATCOM can improve the transient stability of the entire power system.

VIII. CONCLUSIONS

In this study, dynamic and transient stabilities of wind generators are analyzed by using a model system composed of 9-Bus main system and two wind farms composed of fixed speed WTGSs. It is seen that the SVPWM controlled STATCOM connected at the wind farm terminal can enhance both dynamic and transient stabilities of wind generators, even if the capacitor bank of wind generators is reduced by a certain percentage. Moreover, by evaluating the transient stability indexes for a different fault point in the model system, it is also clear that the STATCOM can improve the transient stability of the multimachine power system including wind farms.

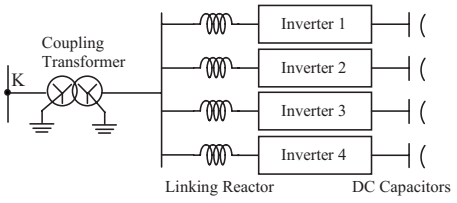

FIG. 26. Schematic diagram of parallel connected inverter topology.

ACKNOWLEDGMENTS

This work was supported by the Grant-in-Aid for JSPS Fellows from Japan Society for the Promotion of Science (JSPS).

APPENDIX: LARGE CAPACITY STATCOM TOPOLOGY

For large capacity system such as a 50 MVARs STATCOM, parallel connected inverter topology can be adopted as shown in Fig. 26.

[1] The Global Wind Energy Council, GWEC Latest News, 2008, "US, China & Spain lead world wind power market in 2007," February, 2008, (Online) http://www.gwec.net/
[2] F. V. Hulle, "Large scale integration of wind energy in the European power supply analysis, issue and recommendations," EWEA, Tech. Rep., December (2005).
[3] L. Gyugyi, IEE Proc.: Gener. Transm. Distrib. **139**(4), 323 (1992).
[4] L. Gyugyi, IEEE Trans. Power Deliv. **9**(2), 904 (1994).
[5] H. F. Wang, F. Li, and R. G. Cameron, IEE Proc.: Gener. Transm. Distrib. **146**(5), 409 (1999).
[6] C. L. Souza, L. M. Neto, G. C. Guimaraes, and A. J. Moraes, in *Power Tech Proceedings, 2001 IEEE Porto* (IEEE, New York, 2001), Vol. 2, p. 6.
[7] Z. Saad-Saoud, J. Chem. Technol. Biotechnol. **145**(5), 511 (1998).
[8] T. Sun, Z. Chen, and F. Blaabjerg, "Flicker mitigation of grid connected wind turbines using STATCOM," Proc. of the 2nd IEE International Conference on Power Electronics, Machines and Drives, PEMD04, 2004 (unpublished).
[9] Z. Chen, F. Blaabjerg, and Y. Hu, "Voltage recovery of dynamic slip control wind turbines with a STATCOM," International Power Electronic Conference (IPEC05), S29–5, 2005, pp. 1093–1100 (unpublished).
[10] S. M. Muyeen, M. A. Mannan, M. H. Ali, R. Takahashi, T. Murata, and J. Tamura, "Stabilization of grid connected wind generator by STATCOM," International Conference on Power Electronics and Drive Systems (IEEE PEDS 2005), Conference CDROM, Malaysia, 2005 pp. 1584–1589 (unpublished).
[11] J. Holtz, Proc. IEEE **82**(8), 1194 (1994).
[12] D. W. Novotny and T. A. Lipo, *Vector Control and Dynamics of ac Drives* (Springer, New York 1996).
[13] J. R. Rodriguez, J. W. Dixon, J. R. Espinoza, J. Pontt, and P. Lezana, IEEE Trans. Ind. Electron. **IE-52**(1), 5 (2005).
[14] K. Zhou and D. Wang, IEEE Trans. Ind. Electron. **IE-49**(1), 186 (2002).
[15] S. Ogasawara, H. Akagi, and A. Nabae, "A novel PWM scheme of voltage source inverters based on space vector theory," Proc. EPE'89, 1989, pp. 1197–1202, (unpublished).
[16] K. Salman and A. L. Teo, IEEE Trans. Power Syst. **18**(2), 793 (2003).
[17] S. M. Muyeen, M. H. Ali, R. Takahashi, T. Murata, J. Tamura, Y. Tomaki, A. Sakahara, and E. Sasano, "A comparative study on transient stability analysis of wind turbine generator system using different drive train models," IET-Proceedings on Renewable Power Generation (IET-RPG), Vol. 1(2), pp. 131–141 (2007).
[18] Federal Energy Regulatory Commission (FERC), United States of America, Docket No. RM05-4-000—Order No. 661, "Interconnection for wind energy," Issued June 2, 2005.
[19] Ireland National Grid, Grid Code Version 2, January, 2007, "Wind farm power station grid code provisions, WFPS1," pp. 213–216.
[20] S. Heier, *Grid Integration of Wind Energy Conversion System* (Wiley, Chicester, 1998).
[21] P. M. Anderson and A. Bose, IEEE Trans. Power Appar. Syst. **PAS-102**(12), 3791 (1983).
[22] P. Kundur, *Power System Stability and Control* (McGraw-Hill, New York, 1994).
[23] PSCAD/EMTDC Manual, Manitoba HVDC Research Center, 1994.
[24] S. M. Muyeen, M. A. Mannan, M. H. Ali, R. Takahashi, T. Murata, and J. Tamura, "Simulation technique & application of space-vector PWM method in PSCAD/EMTDC," CD Record of International Conference on Information & Communication Technology (ICICT 2007), Reference No. 041, Dhaka, Bangladesh, March 7–9, 2007.
[25] Working Group on Prime Mover and Energy Supply Models for System Dynamic Performance Studies, IEEE Trans. Power Syst. **6**(2), 753 (1991).
[26] Working Group on Prime Mover and Energy Supply Models for System Dynamic Performance Studies, IEEE Trans. Power Syst. **7**(12), 167 (1992).
[27] IEEE Recommended Practice for Excitation System Models for Power System Stability Studies, IEEE Std. 421.5-1992.
[28] I. Zubia, X. Ostolaza, G. Tapia, A. Tapia, and J. R. Saenz, "Electrical fault simulation and dynamic response of a wind farm," Proceedings of the IASTED International Conference Power and Energy Systems, 2001, pp. 595–600, (unpublished).
[29] S. M. Muyeen, M. H. Ali, R. Takahashi, T. Murata, and J. Tamura, IEEJ Trans. Power Energy **126-B**(08), 742 (2006).
[30] M. Yagami, S. Shibata, T. Murata, and J. Tamura, IEEJ Trans. Power Energy **123**(2), 133 (2003).